

ORIGINAL RESEARCH PAPER

Green synthesis of ZnO nanoparticles and their photocatalyst degradation and antibacterial activity

G. Kamarajan¹, D. Benny Anburaj^{1*}, V. Porkalai², A. Muthuve³, G. Nedunchezian⁴, N. Mahendran⁵

¹ PG and Research Department of Physics, D.G. Government Arts College (Affiliated to Bharathidasan University, Trichy), Mayiladuthurai, Tamil Nadu-609001, India.

² Department of Physics, Nethaji Subash Chandra Bose College for Co-ed (Affiliated to Bharathidasan University, Trichy), Senthemangalam, Tamilnadu-614001, India.

³ PG and Research Department of Physics, T.B.M.L. College (Affiliated to Bharathidasan University, Trichy), Porayar, Tamil Nadu-609307, India.

⁴ PG and Research Department of Physics, Thiru. Vi. Ka. Government Arts College (Affiliated to Bharathidasan University, Trichy), Thiruvarur, Tamil Nadu-61003, India.

⁵ PG and Research Department of Physics, Idhaya College for Women (Affiliated to Bharathidasan University, Trichy), Kumbakonam, Tamil Nadu-612001, India.

Received: 2022-02-13

Accepted: 2022-04-01

Published: 2022-05-01

ABSTRACT

The current study aimed to synthesize nanoparticles of Zinc oxide (ZnO) using the extract of *Acalypha indica* leaves and their photocatalyst degradation and antibacterial properties were also measured. The biosynthesized nanoparticles were analyzed using XRD, UV-visible, FT-IR, and SEM with EDAX, DLS, PL, and Zeta potential analysis. The synthesized nanoparticles had a mean size of 16 nm measured by XRD which was highly pure, and their spherical shape was confirmed by SEM. The UV-visible confirmed that ZnO nanoparticles have a direct band gap energy is 3.34 eV. The measured zeta size and potential of synthesized nanoparticles were 46 nm and -27 mV, respectively, determined by the DLS technique can be considered moderately stable colloidal solutions. The FT-IR analysis confirmed the presence of functional groups in the leaf extract and the ZnO nanoparticles. The biosynthesized ZnO nanoparticles have a homogeneous spherical morphology and the average particle is 35 nm. The PL analyses performed on synthesized nanoparticles showed a sharp blue band at 362 nm, which was attributed to the defects of structure in ZnO crystals. During natural sunlight illumination, ZnO nanoparticles demonstrated notable degradation of the dye methyl blue (MB). At 90 min of illumination, the degradation efficiency achieved was 96 %. Antibacterial properties were observed for synthesized nanoparticles against four bacterial strains, including *Bacillus subtilis*, *Staphylococcus aureus*, *Pseudomonas aeruginosa*, and *Escherichia coli*. The highest zone of inhibition was observed against *Escherichia coli* (25.2 mm). Overall, these studies indicate that *Acalypha indica* is a good sell for planting, and has the greatest chance of being used to develop nanoparticles for protection against environmental pollution and human health.

Keywords: Zinc oxide, green synthesis, *Acalypha indica*, XRD, photocatalyst, antibacterial.

How to cite this article

Kamarajan G., Benny Anburaj D., Porkalai V., Muthuve A., Nedunchezian G., Mahendran N. Green synthesis of ZnO nanoparticles and their photocatalyst degradation and antibacterial activity. J. Water Environ. Nanotechnol., 2022; 7(2): 180-193.

DOI: 10.22090/jwent.2022.02.006

INTRODUCTION

The nanotechnology sector stands as one of the most promising technologies for manipulating

nanoscale for a wide range of science disciplines, including ceramic materials, cosmetics, food, and pharmaceuticals [1]. Nanoparticles are a promising strategy to improve health and industrial applications due to their exceptional properties,

* Corresponding Author Email: bennyburaj@gmail.com



This work is licensed under the Creative Commons Attribution 4.0 International License.

To view a copy of this license, visit <http://creativecommons.org/licenses/by/4.0/>.

such as small size, high adsorption, high catalytic activity, large surface area, a large number of reactive sites, and chemical stability [2]. Since metal and metal oxide nanoparticles have many valuable properties, including catalytic, optical, electrical, and magnetic properties, they have become very appealing materials in several fields over the past few years [3]. Metal and metal oxide nanoparticles are used in various fields such as solar cells, laser deflectors, photonics, water treatment, biomedicine, transparent, piezoelectric, catalyst and gas sensors [4,5]. Metal oxide nanoparticles, especially ZnO nanoparticles, seem to be particularly effective for antibacterial activities, eco-friendly agrochemicals, photocatalyst degradation, and photocatalysis for environmental remediation [6]. Due to their high stability, ZnO nanoparticles are considered probable next-generation materials as biocidal and fumigating agents. This stability is ascribed to them being more versatile than organic-based decontaminators and anti-microbial agents [7]. As a semiconductor, ZnO has a wideband gap (3.37 eV) and an exciton binding energy of 60 meV, which is an efficient source of excitonic blue radiation. As a result of its inherent ability to absorb UV irradiation, ZnO has been accepted by the food and drug administration (FDA) for use in sunscreens [8]. To synthesize the ZnO nanoparticles, several physical and chemical strategies were used, whereas sol-gel [9], chemical precipitation [10], laser ablation [11], chemical vapor deposition [12], pyrolysis [13], hydrothermal [14], and solvothermal route [15] have been used. The above methods used to synthesize nanoparticles are complex, costly processes that produce hazardous toxic wastes that are harmful to both humans and the environment [16], and also limited in biomedical applications because of the toxic chemicals required. To overcome these disadvantages, it is imperative to explore alternative green sources. The process of green synthesis utilizes a variety of natural sources, including plants, bacteria, algae, and fungi [17]. The biosynthesized nanoparticles are nontoxic, biocompatible, and eco-friendly [18]. The natural extract may contain bioactive compounds that may bind to the surface of the nanoparticles, and their density will be dependent on synthesis parameters [18]. Phytochemicals, such as flavones, phenols, amino acids, sugars, carotenes, amides, aldehydes, ketones, etc., present in plants have been widely used for green synthesis. Nanoparticles and

biological materials interact to control the surface coatings of the fabricated materials [19]. There have been numerous reports on the synthesis of ZnO nanoparticles with leaf extract such as *Solanum nigrum* [9], *Cinnamomum verum* [20], *Azadirachta indica* [21], *Passiflora caerulea* [22], *Curry* [16], *Moringa oleifers* [23], and their antibacterial activity. *Acacia arabica* leaf extract is used to biosynthesize ZnO nanoparticles for antimicrobial and antioxidant activity.

The traditional medicinal plant of south India, *Acalypha indica* (Euphorbiaceae), contains bio-reductants and stabilizers. There are several medicinal applications of these plants, including anti-inflammatory, antifungal, anticancer, and antibacterial effects, which are useful in treating asthma, rheumatism, and pneumonia. The leaf of *Acalypha indica* shows a significant number of proteins, carbohydrates, alkaloids, felonies, tannins, phenolics, terpenoids, and amino acids [24]. Nanoparticles of copper oxide [25], titanium oxide [26], and silver oxide [27] have been synthesized using *Acalypha indica* leaf extract. It has been suggested that phenols, aldoses, and proteins are responsible for the creation of metal oxide nanoparticles. In our study, we synthesize ZnO nanoparticles using the leaf extract of *Acalypha indica* for the first time. It is easier to use, less expensive, and more eco-friendly than the conventional method. The present study utilized *Acalypha indica* leaf extract for reducing zinc nitrate to ZnO nanoparticles which were synthesized and characterized using several techniques: UV-Visible spectroscopy (UV-vis), Photoluminescence (PL), Scanning electron microscopy (SEM), Zeta potential (ZE), X-ray diffraction (XRD), Fourier transform infrared spectroscopy (FT-IR), Energy-dispersive X-ray spectroscopy (EDX) and Dynamic light scattering (DLS) analysis. Also, nanoparticles produced as photocatalysts are utilized to degrade organic dye and inhibit microorganisms that cause human disease.

MATERIAL AND METHODS

Materials

The chemicals such as Zinc acetate dihydrate ($Zn(CH_3COO)_2 \cdot 2H_2O$) and all the chemicals and reagents were procured since Merck chemical reagent co distilled this work purchased since the leaves of *Acalypha indica* plant together form in and around the garden, Nagapattinam, Tamil Nadu, India.

Plant leaf collection

Fresh leaves of plants that is, *Acalypha indica* were collected from Nagapattinam. The leaves were identified and authenticated by the Department of Agriculture, Annamalai University in Tamil Nadu. To remove dust particles from the surface of the leaves, they were twice washed with tap water and then repeatedly washed in double-distilled water. The washed leaves were then shade dried for five days. Then, 20 gm of dried leaves were crushed and 50 mL of distilled water was added. After that, a magnetic stirrer was used to stir the mixture, then the mixture was heated for 1 h at 60°C. When the mixture displayed a yellow color, it was filtered using Whatman filter paper. As a result, nanoparticles of ZnO were prepared from the exact solution.

Biosynthesis of ZnO nanoparticles

The ZnO nanoparticles were biosynthesized by following the Sol-gel method designated by Muthuvel et al. [9]. Briefly, it was prepared by stirring 2 M zinc acetate in 50 mL of deionized water for 30 min at 85°C. To prepare a NaOH solution, 4 gm NaOH powder was added to 50 mL of distilled water and stirred simultaneously at 85°C for 30 min. The two solutions were then vigorously stirred together. The 15 mL leaf extract was mixed with the solution drop by drop during this stirring process. After stirring continuously for 2 h using a magnetic stirrer, a white precipitate was obtained. To remove the impurities, the precipitate was filtered and repeatedly washed with distilled water followed by ethanol. After the precipitate was dried at 400°C for 4 h and the obtained ZnO powder was subjected to further characterization.

Characterization of synthesized nanoparticles

To collect X-ray diffraction data for the formed samples, SHIMADZU-XRD 6000 analytical diffractometers were used. We measure UV absorbance and photoluminescence with a Shimadzu UV-VIS-260 system. The morphology of the synthesized nanoparticles was examined using scanning electron microscopy (Hitachi S-4500 machine). DLS and zeta potential were measured by Malvern Zeta Sizer (ZS 90, USA). Measurements were made with a Bruker tensor 27 FT-IR spectrometer using Fourier transform infrared spectra.

Photocatalyst activity

To assess the photocatalyst activity of ZnO

nanoparticles under sunlight, MB was selected as the model contaminant for photocatalyst degradation. The stock solution of 50 ppm MB in distilled water was prepared by dissolving of distilled water. Using a UV-vis spectrometer with maximum absorption at 661 nm, the concentration of MB at the initial concentration was determined. Thereafter, 100 mL of stock solution will be poured into a 100 mL beaker, followed by 100 mg of ZnO nanoparticles. After exposing the solution to sunlight for some time, 3 mL, of the solution was withdrawn and the suspended ZnO powder was centrifuged at 6000 rpm for 15 min. after the solution was degraded, the absorbance was measured. This equation was used to estimate the degradation percentage of the photocatalyst [28];

$$\text{Degradation percentage} = \frac{C_o - C_t}{C_o} \times 100 \quad (1)$$

where, Co is the dye concentration before degradation, and Ct is the dye concentration at different times t.

Bacterial activity

The antibacterial activity of *Acalypha indica* leaf extract and biosynthesized ZnO nanoparticles were established using the disc diffusion method on four types of bacteria: *Bacillus subtilis*, *Staphylococcus aureus*, *Pseudomonas aeruginosa*, and *Escherichia coli*. The samples of 5 and 10 µg/mL concentration were poured onto ach disk and placed on Muller Hinton agar plates. The antibiotic dis Ciprofloxacin was used as the positive control. Incubation was carried out at 35°C for 24 h. By forming an inhibitory zone around the wells, the antibacterial activity of the samples was determined.

RESULTS AND ANALYSIS

XRD analysis

The XRD pattern was used to determine the crystallinity and phase of synthesized ZnO nanoparticles (Fig. 1). The peak positions with 2θ values of 31.7°, 34.9°, 36.4°, 53.8°, 66.4°, 75.5°, and 82.6° can be assigned to planes (100), (022), (101), (102), (110), (103) and (200) which corresponds to hexagonal Wurtzite structure of ZnO nanoparticles (JCPDS card no:5-0664). It is evident from the quality of peaks that the ZnO nanostructures are well-crystalline. The XRD result obtained were very similar to what had previously been recorded [29]. The XRD pattern does not show any additional peaks, demonstrating the high purity of the ZnO

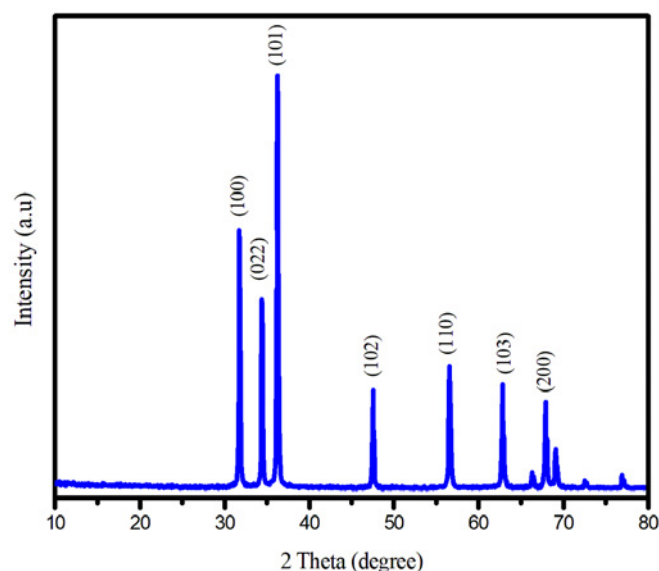


Fig. 1. XRD pattern of biosynthesized ZnO nanoparticles

Table 1. Structural parameters of the biosynthesized ZnO nanoparticles

Position ($^{\circ}$ 2th)	Planes	FWHM left ($^{\circ}$ 2th)	Average crystal size (nm)	Average dislocation density (δ) $\times 10^{15}$	Average micro strain (ϵ)
31.7	(100)	0.1476			
34.9	(022)	0.1456			
36.4	(101)	0.1968			
53.8	(102)	0.2952	16.2	5.678	0.01345
66.4	(110)	0.1476			
75.5	(103)	0.2952			
82.6	(200)	0.1476			

nanoparticles This suggests anisotropic growth and a preferred orientation of crystallites, based on the relatively high intensity of the (101) peak. Further analysis of the XRD spectrum is conducted to establish crystal structural parameters such as dislocation density (δ), the crystallite size (D), and microstrain (ϵ) as described in Eqs 2-4 [9].

$$D = \frac{0.89\lambda}{\beta \cos\theta} \quad (2)$$

$$\epsilon = \frac{\beta \cos\theta}{4} \quad (3)$$

$$\delta = \frac{1}{D^2} \quad (4)$$

Where, λ is the wavelength of the X-ray source (0.1541 nm), D is the average crystalline size (nm), the angle of Bragg's diffraction is θ ,

and the angular peak width at half maximum is given by β in radians along with the (1 1 1) plane. The crystalline size of biosynthesized ZnO nanoparticles has been calculated to be around 16.2 nm, as well as the dislocation density and microstrain, which are about 5.678 and 0.1345, respectively. Table 1 shows the structural parameters values of green synthesized ZnO nanoparticles. The crystalline size of the biosynthesized ZnO nanoparticles from *Acalypha indica* leaf extract is very small when compared to other leaf extracts (*Cinnamomum verum*, *Azadirachta indica*, and *Passiflora caerulea*) used in synthesizing ZnO nanoparticles [20, 21, 22] and also *Acalypha indica* leaves extract used biosynthesized iron and silver oxide nanoparticles [30, 27]. The present study has a very small crystallite size of 16 nm, and this will greatly improve antibacterial activity and photocatalysis.

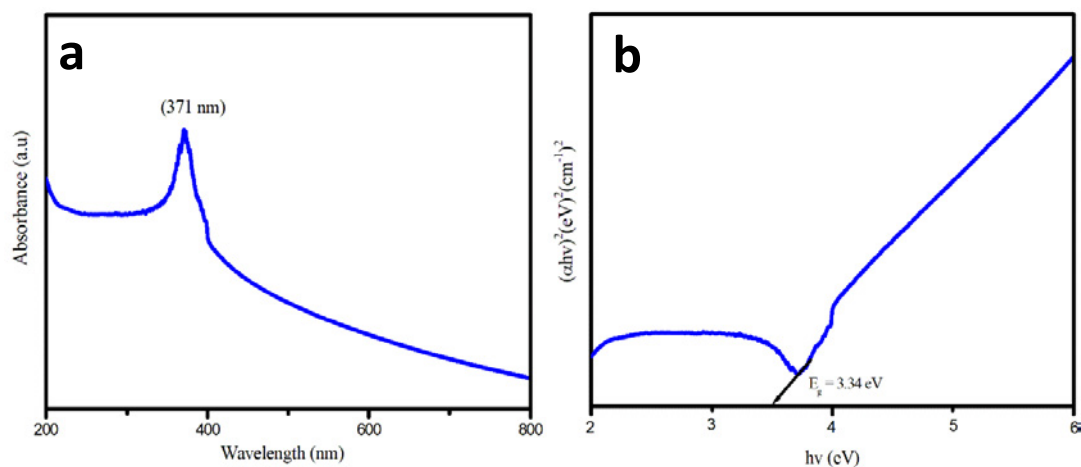


Fig. 2. a) UV-visible spectra and b) band gap energy of biosynthesized ZnO nanoparticles

UV-visible analysis

UV-Vis absorption spectroscopy was used to confirm the optical properties of the biosynthesized ZnO nanoparticles. Fig. 2a shows the UV-Vis absorption spectrum of synthesized nanoparticles from 200–800 nm. The figure shows absorption bands at 371 nm that confirm the presence of ZnO nanoparticles in culture filtrate. Therefore, the absorption spectrum of ZnO nanoparticles will show a strong shift towards blue, indicating that their size is less than the exciton Bohr radius [31]. ZnO nanoparticles are characterized by the blue peak, while nanoscale confinement is indicated by a blue shift. Satheshkumar et al. also obtained similar results for the absorption band, similarly [16], Jamdagni et al., ZnO nanoparticles UV-vis spectrum range between 330–390 nm [32]. The UV spectrum range of ZnO nanoparticles was also measured at 380 nm by Muthuvel et al. [9]. The band gap energy of ZnO nanoparticles synthesized was determined by UV-vis spectroscopy based on the following Eq [28];

$$(\alpha h\nu)^2 = B (h\nu - E_g)^{1/2} \quad (5)$$

where B is a constant, h is the Planck constant ($6.626 \times 10^{-34} \text{ J Hz}^{-1}$), $h\nu$ is photon energy, E_g is the optical band gap energy and α is the absorption coefficient. The band gap energy of synthesized nanoparticles is displayed in Fig 2b. The observed band gap energy of ZnO is 3.34 eV, lower than the band gap of bulk ZnO due to quantum confinement effects [33]. The ZnO nanoparticles synthesized

in the present study have a band gap energy in good agreement with that found in Vijayakumar et al. [34]. The present band gap energy is very low for the ZnO nanoparticles synthesized by some chemical methods [12, 14, 15]. The present work demonstrates that ZnO nanoparticles can be obtained by biological means from small band gap values and that this greatly enhances their antibacterial properties.

DLS and Zeta potential analysis

Nanoparticles undergoing Brownian movement are measured by measures of their time-dependent scattering of light, the particle size distribution was determined using dynamic light scattering analysis [9]. In colloidal solution, dynamic light scattering is widely used to ration the shell thickness of capping agents or stabilizers omnipresent metallic nanoparticles, as well as the size of the metallic core. Fig. 3a shows the DLS pattern of biosynthesized ZnO nanoparticles using *Acalypha indica* leaf extract. The size distribution of synthesized nanoparticles is found to be 46 nm. Furthermore, the negative zeta potential of ZnO nanoparticles, which is found to be -27.47 mV, further confirms the stabilization of synthesized nanoparticles (fig 3b). Particles with zeta potential above +30 mV or below -30 mV are considered stable. With a zeta potential of -27.47 mV, the ZnO nanoparticles synthesized via biosynthesis at 400 °C are very stable. The high negative value of the zeta potential correlated with the presence of negatively charged groups on the surface of the nanoparticles. This reduction of

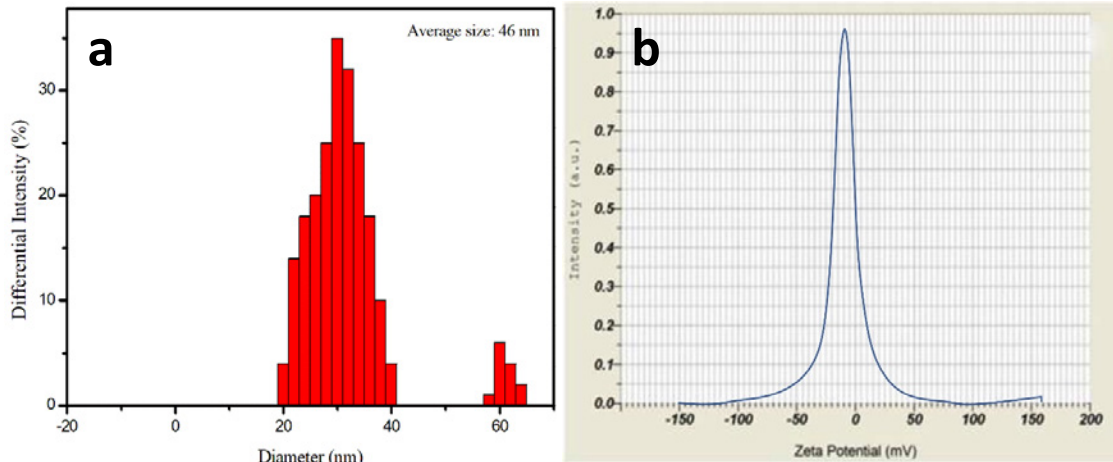


Fig. 3. a) DLS pattern b) Zeta potential of biosynthesized ZnO nanoparticles

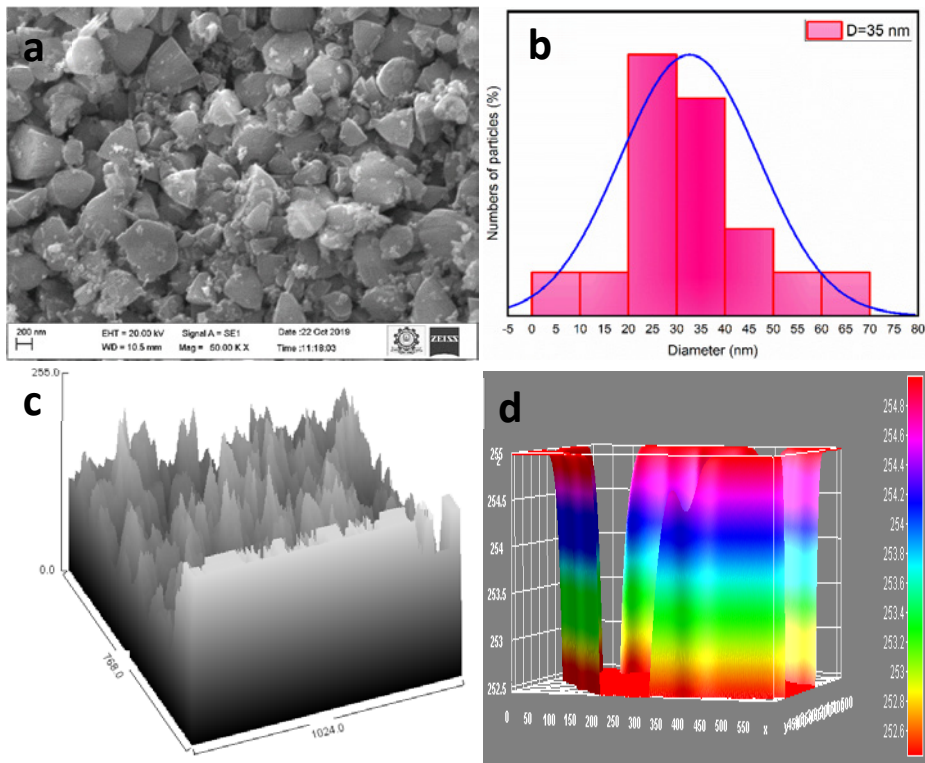


Fig. 4. a) SEM image b) particles size distribution c-d) surface plot analysis of biosynthesized ZnO nanoparticles

metal ions and stabilization of nanoparticles could be caused by protein and flavonoids in the leaf extract. There are similar kinds of results reported by Chaudhuri et al. [35].

SEM analysis

The SEM was used to detect the morphology and size of the biosynthesized nanoparticles.

The SEM image of synthesized nanoparticles is shown in Fig 4 (a). The figure shows, that the biosynthesized ZnO nanoparticles have a homogeneously spherical morphology. Upon closer inspection, several aggregates of nanoparticles can be seen in the agglomerated lump. Particles are agglomerated, and some individual crystals can be seen in Fig 4(a). In Fig 4(b), the histogram of

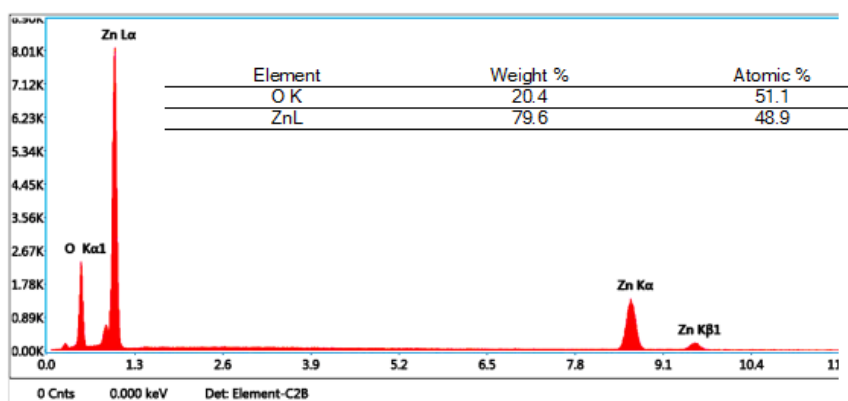
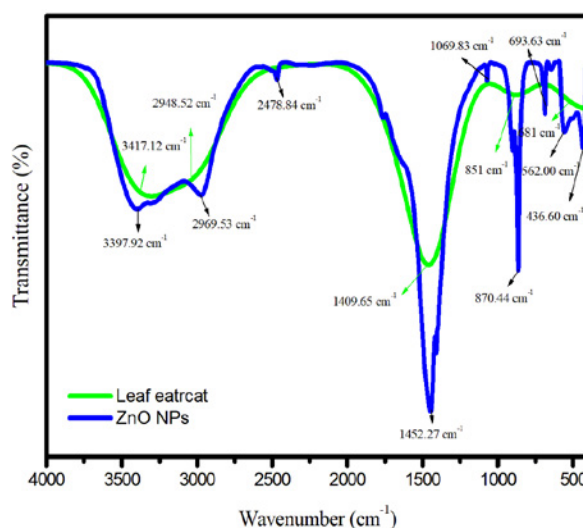


Fig. 5. EDS spectrum of the biosynthesized ZnO nanoparticles

Fig. 6. FT-IR spectra of *Acalypha indica* leaf extract and biosynthesized ZnO nanoparticles

particle sizes distribution shows that the mean diameter of ZnO nanoparticles is 35 nm. The EDX result shown in Fig 5 further confirms the presence of zinc nanoparticles in oxide form, indicating that the biosynthesis of ZnO nanoparticles provides an effective way to process inorganic matter. Fig. 4 (c-d) shows a surface plot analysis of synthesized nanoparticle images. It has been demonstrated that biosynthesized ZnO nanoparticles have the highest porosity, thus allowing more dye molecules to absorb, which would improve the performance of the photocatalyst.

FT-IR analysis

The FT-IR analysis can be used to identify the possible reducing and stabilizing biomolecules. Wave number range between 400 to 4000 cm^{-1} was used for FT-IR analysis. Fig. 6 shows the FT-

IR spectra of the *Acalypha indica* leaf extract and biosynthesized ZnO nanoparticles. The FT-IR spectrum of *Acalypha indica* leaf extract exhibited several peaks at 3417.12, 2948.52, 2487.52, 1409.65, 851.69, and 681.87 cm^{-1} . The peaks at 3417.12 (O-H), 2948.52 (CH_2), 2487.52 (stretching mode of C-H), 1409.65 (bending mode), 800-500 (RC=OO) cm^{-1} are associated with phenols, alkaloids, resins, saponins, tannins, and flavonoids compounds, respectively [26, 27]. As a result of the functional group's analysis, *Acalypha indica* leaf extract contained carboxylic and amino groups. It is the responsibility of the groups to bio-transform zinc ions into zinc oxide nanoparticles. In synthesized ZnO nanoparticles, the major absorption bands are 3397.92, 2969.53, 2478.84, 1452.27, 870.44 and 600-400 cm^{-1} . The O-H stretching vibrations are present in flavonoids and phenolics, giving rise to

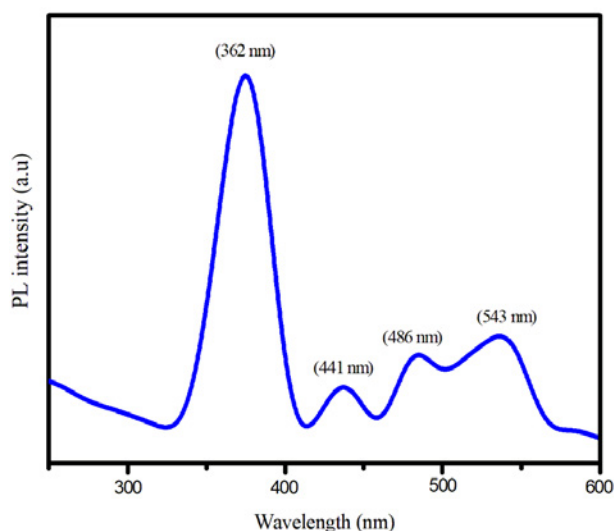


Fig. 7. PL spectra of biosynthesized ZnO nanoparticles

the broad absorption peak, 3397.32 cm^{-1} [16]. A peak at 296.53 cm^{-1} is attributed to the C-H stretch of the alkane functional group [9]. An alkyl peak was assigned to the O-H group at, 2478.84 cm^{-1} . The peak at, 1452.27 cm^{-1} is due to the C=C stretch of the aromatic ring system [36]. Around 870 cm^{-1} , the absorption peak is probably in the O-H functional group [37]. ZnO is considered to have a stretching mode absorption peak between 400 to 600 cm^{-1} . The biosynthesized ZnO nanoparticles exhibit absorption bands between 400 to 600 cm^{-1} [38]. As a consequence, phytochemicals show a role in the biotransformation of nitrates to oxides. Biosynthesized ZnO nanoparticles showed new characteristic peaks as compared to pure ZnO nanoparticles [9]. 2948.52 and 1409.65 cm^{-1} were peaks created by flavonoids and phenolics of leaf extract molecules, confirming the presence of phytochemicals on ZnO nanoparticles. Plant phytochemicals reduce the size of nanoparticles during their formation. Mahendra et al. and Vijayakumar et al. also observed similar findings [38, 34].

PL analysis

The study of the PL, a property of biosynthesized ZnO nanoparticles, is interesting because it can give valuable insights into the quality and purity of the material. ZnO nanoparticles are shown in Fig 7 as PL spectra at room temperature. An excitation wavelength of 320 nm was used for the PL measurements. The PL spectra of ZnO

nanoparticles at room temperature show four main peaks, 362 , 441 , 486 , and 543 nm . It correlates with the Near band emission of ZnO at 362 nm . The excited electron of a valence band recombines with the holes by radiative recombination [39]. A weak peak at 441 nm was attributed to irradiative excitation annihilation, and a weaker peak at 486 nm to defects in the band gap produced during sample preparation, such as oxygen vacancies [40]. The 543 nm , green band may correspond to a transition between interstitial and vacancy oxygen [41]. This study showed that *Acalypha indica* leaf extract can synthesize nanoparticles that have intrinsic defects, oxygen vacancy, and surface defects sites that can enhance antimicrobial and photocatalytic activities.

Photocatalysts activity

An investigation of the photocatalytic activity of biosynthesized ZnO nanoparticles under sunlight irradiation was carried out using MB dye degraded in an aqueous solution. Fig. 8(a) shows the change in MB absorption spectrum during photocatalytic degradation using ZnO nanoparticles at different radiation times, ranging between 0 to 90 min . After 90 min of irradiation, 96% of the MB had degraded. It was also visually observed that the dye solution gradually turned from blue to colorless due to the photodegradation of MB. The MB dye shows strong absorption maxima at 661 nm due to the chromophore group, and it gets weaker as the irradiation time increases and becomes invisible

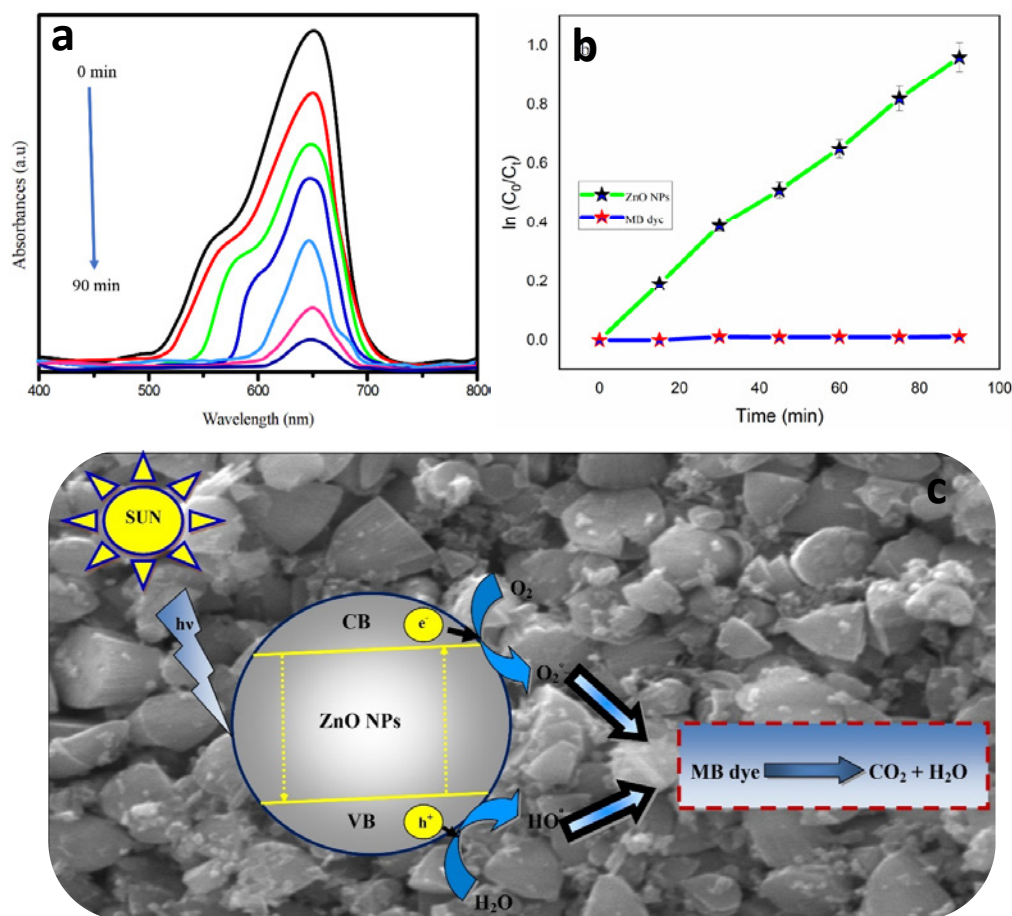


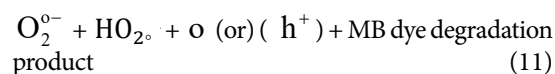
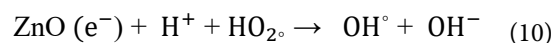
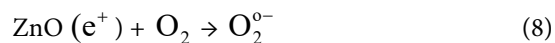
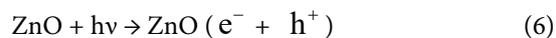
Fig. 8. (a) UV-vis absorption spectra of MB dye with respect to irradiation time versus; (b) rate constant (K) and regression (R²) and (c) Mechanism for photodegradation of MB dye of biosynthesized ZnO nanoparticles

within 90 min, indicating that the chromophore in MB molecules is completely removed. Metal oxide nanoparticle size plays a significant part in photocatalyst reduction since a decrease in the size of biosynthesized ZnO nanoparticles improves the adsorption of reactants on impetus surfaces and promotes corrosion. Increasing the surface area of the particles will therefore increase the effectiveness of the catalyst.

Mechanism of photocatalyst activity

The electron in the valence band of the synthesized ZnO nanoparticles absorbs energy as visible light is irradiated and moves to the conduction band (CB), departure a hole in the valence band (VB) (Fig 8c). This leads to the formation of electron-hole pairs, which rise to the surface. Water molecules generate hydroxyl radical ($\cdot OH$) when the holes corrode the OH^-

ions, while ambient oxygen is oxidized by the electrons to produce superoxide radius ($\cdot O_2^-$). The photocatalyst reaction mechanism is depicted below [9];



Biosynthesised ZnO nanoparticles are

Table 2. The comparative assessment of photocatalytic activity of synthesized ZnO nanoparticles with existing reports

Name of source	Part of the source	Size of NPs (nm)	Reaction time (min)	Degradation efficiency (%)	Dye	Light source	References
<i>Acalypha indica</i>	Leaf	16	90	96	MB	Sunlight	This work
<i>Peltophorum pterocarpum</i>	Leaf	11	120	95	MB	Sunlight	[43]
<i>Sambucus ebulus</i>	Leaf	--	120	80	MB	UV light	[44]
<i>Eriobotria japonica</i>	Seed	14	120	52	MB	UV light	[45]
<i>Bridelia retusa</i>	Leaf	11	165	94	RhB	Sunlight	[46]
<i>Cyanometra ramiflora</i>	Leaf	13	200	98	RhB	Sunlight	[47]

primarily definite by the degradation of color dyes that determine their surface charge, crystallite size, and structure. As a result of photoinduced organic reactions on the catalyst superficial, a photocatalyst system is formed. In the presence of light, electron pores on the surface of the catalyst promote redox reactions, resulting in $^{\circ}\text{O}_2^-$ and OH^- . Due to their powerful photocatalytic properties, these radicals degrade toxins in wastewater.

Kinetic study

Based on pseudo-first-order reaction kinetics, we calculated the degradation rate of MB dye in the presence of synthesized ZnO nanoparticles [28].

$$\ln(A_0/A_t) = -kt \quad (12)$$

where t is time (min), in the first order, Pseudo rate constant k , A_0 , and A_t are absorptions of MB dye at time t to zero, respectively. As a function of irradiation duration, in (A_0/A_t) is 1.04476 min^{-1} for MB dye. Additionally, the fitting correlation coefficient (R^2) is calculated as 0.9952. A_0/A_t values decrease with time, but MB dye degradation percentages increase with time (Fig 8b). As shown in Table 2, the ZnO nanoparticles synthesized from *Acalypha indica* leaf extract showed enhanced photocatalytic activity in organic dye than any other leaves extract used to synthesize ZnO nanoparticles.

Antibacterial activity

Figs. 9 shows the antibacterial activity of aqueous leaf extract of *Acalypha indica* and biosynthesized ZnO nanoparticles were investigated by both Gram-positive (+Ve) and gram-negative (-Ve) bacteria by disk diffusion method. Table 3 shows the diameter of the zone of inhibition (mm). A linear increase in the size of the inhibition zone occurs with an increase in sample concentration, as shown in Table 3. The leaf extracts were

minimally active at higher concentrations with zones of inhibition ranging from 15, 12, 11, and 8 mm for *Escherichia coli*, *Pseudomonas aeruginosa*, *Staphylococcus aureus*, and *Bacillus subtilis*. The phytochemicals in *Acalypha indica* leaf extract may be responsible for the very tiny antibacterial activities present in it. Based on the antibacterial activity results, biosynthesized ZnO nanoparticles were effective against all tested bacteria. At higher concentrations, *Bacillus subtilis* (21 mm), *Staphylococcus aureus* (22 mm), *Pseudomonas aeruginosa* (23 mm) and *Escherichia coli* (25 mm) were found to be in the zone of inhibition. Gram-negative bacteria are more susceptible to biosynthesized ZnO nanoparticles than gram-positive microbes. There was a difference in the cell wall properties of Gram-positive and Gram-negative bacteria, with Gram positives having an impenetrable outer cell sheath layer, which made them immune to ZnO nanoparticles. In addition, it was proposed that gram-negative bacteria were immune to nanoparticles due to lip polysaccharides on their cell walls. In a report by Mahendra et al. [38], the antibacterial activities of synthesized nanoparticles were testified to be extra active against gram-negative bacteria than gram-positive microorganisms. ZnO nanoparticles have a variety of mechanisms for causing antibacterial action, the most common of which is the production of ROS and the proclamation of Zn^{2+} , which result in cubicle impairment and death in bacteria [21]. Moreover, because ZnO nanoparticles are cations, they can electrostatically attribute to the negatively charged surface of bacteria, causing them to become damaged. The biosynthesized ZnO nanoparticles exhibited greater antibacterial activities in the current study because of their small size and stability (Table 4). The antibacterial activities of smaller nanoparticles are greater than that of bulk nanoparticles due to their higher surface area and responsiveness. Among the biosynthesized ZnO

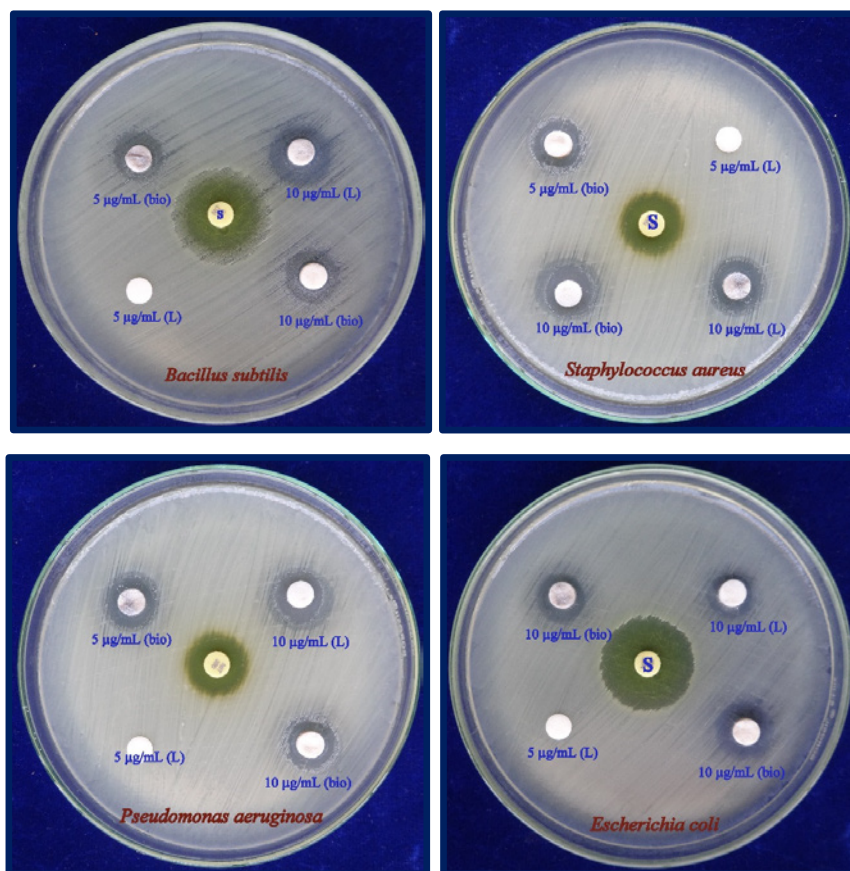


Fig. 9. Antibacterial activity of *Acalypha indica* leaf extract and biosynthesized ZnO nanoparticles against human pathogenic bacteria at different concentrations

Table 3. Antibacterial activity of *Acalypha indica* leaf extract and biosynthesized ZnO nanoparticles against human pathogenic bacteria

Bacteria's	Zone of inhibition (mm)				Standard
	5 µg/mL		10 µg/mL		
	Leaf	Bio ZnO	Leaf	Bio ZnO	
<i>Bacillus subtilis</i>	3	10	8	21	25
<i>Staphylococcus aureus</i>	5	11	11	22	25
<i>Pseudomonas aeruginosa</i>	5	12	12	23	25
<i>Escherichia coli</i>	6	13	15	25	26

Table 4. Comparison of obtained antibacterial results of prepared samples with the literature

Name of source	Parts of source	Zone of inhibition (mm)				References
		<i>Bacillus subtilis</i>	<i>Staphylococcus aureus</i>	<i>Pseudomonas aeruginosa</i>	<i>Escherichia coli</i>	
<i>Acalypha indica</i>	Leaf	21	22	23	25	
Curry	Leaf	--	19	20	22	[16]
<i>Solanum nigrum</i>	Leaf	17	15	19	17	[9]
<i>Passiflora caerulea</i>	Leaf	--	11	--	13	[20]
<i>Pichia kudriavzevii</i>	Leaf	8	9	--	9	[48]
<i>Trifolium pratense</i>	Leaf	--	12	23	31	[49]

nanoparticles with an average crystallite size of 3 nm, Muthuvel et al. [9] observed higher inhibitory activities against *Pseudomonas aeruginosa* and *Escherichia coli* microorganisms. In addition, they found ZnO nanoparticles inhibited *Escherichia coli* growth at a comparatively low concentration of 10 g/mL, which was estimated to be size-dependent [42].

CONCLUSION

In conclusion, we have developed a procedure for the synthesis of ZnO nanoparticles with the use of *Acalypha indica* leaf extract that is environmentally benign and economically, efficient and safe. The XRD results showed that the particles are hexagonal crystalline, and optical properties indicated that the ZnO band gap energy is 3.34 eV. The DLS and ZE analysis showed that the particles were 46 nm in size and had a negative zeta potential of -27.47 eV, suggesting greater stability. FT-IR results revealed that flavonoids and phenolics in *Acalypha indica* leaf extract might have contributed to the synthesis of nanoparticles. A photodegradation of MB dye was used to evaluate the photocatalytic activity of biosynthesized ZnO NPs. Biosynthesized ZnO nanoparticles demonstrated outstanding photocatalytic performance, as evidenced by 96% degradation of MB dye under natural sunlight. The antibacterial activity of biosynthesized ZnO nanoparticles is probably inhibited by their negatively charged surface against Gram-negative bacteria, particularly *Escherichia coli*. In the future, bio-synthesized ZnO nanoparticles have the potential for a greater number of applications in sensors, catalysts, and biomedicine.

CONFLICT OF INTEREST

The authors declare that they have no conflict of interest

DECLARATIONS OF INTEREST

None

REFERENCES

- Akın N, Mutlu Danacı H (2021) An investigation into the architectural use of nanotechnology in the context of the titanium dioxide, Environ Sci Pollut Res 28: 64130–64136.
- Zhuang L, Ge L, Yang Y, Li M, Jia Y, Yao X, Zhu Z (2017) Ultrathin Iron-Cobalt Oxide Nanosheets with Abundant Oxygen Vacancies for the Oxygen Evolution Reaction, Adv. Mater 29:1606793.
- Prochowicz D, Kornowicz A, Lewiński J (2017) Interactions of Native Cyclodextrins with Metal Ions and Inorganic Nanoparticles: Fertile Landscape for Chemistry and Materials Science, Chem Rev 117:13461–13501.
- Muthuvel A, Said NM, Jothibas M, Gurushankar K, Mohana V (2021) Microwave-assisted green synthesis of nanoscaled titanium oxide: photocatalyst, antibacterial and antioxidant properties, J Mater Sci Mater Electron 32:23522–39
- Jayanthi PJ, Punithavathy IK, Jeyakumar SJ, Elavazhagan T, Muthuvel A, Jothibas M (2022) Influence of temperature on the structural, optical, morphological and antibacterial properties of biosynthesized silver nanoparticles, Nanotechnol Environ Eng 8.
- Nguyen DTC, Le HTN, Nguyen TT, Nguyen TTT, Bach LG, Nguyen TD, Tran TV (2021) Multifunctional ZnO nanoparticles bio-fabricated from *Canna indica* L. flowers for seed germination, adsorption, and photocatalytic degradation of organic dyes, J Hazard Mater 420:126586.
- hmad W, Kalra D (2020) Green synthesis, characterization and anti-microbial activities of ZnO nanoparticles using *Euphorbia hirta* leaf extract, J King Saud Univ Sci 32:2358–64.
- Adler BL, DeLeo VA (202) Sunscreen Safety: A Review of Recent Studies on Humans and the Environment, Curr Dermatol Rep 9:1–9.
- Muthuvel A, Jothibas M, Manoharan C (2020) Effect of chemically synthesis compared to biosynthesized ZnO-NPs using *Solanum nigrum* leaf extract and their photocatalytic, antibacterial and in-vitro antioxidant activity, Nanotechnol Environ Eng (2):103705
- N. Goswami N, Sharma DK (2010) Structural and optical properties of unannealed and annealed ZnO nanoparticles prepared by a chemical precipitation technique, Physica E Low Dimens Syst Nanostruct 42:1675–1682.
- Chen W, Yao C, Gan J, Jiang K, Hu Z, Lin J, Xu N, Sun J, Wu J (2020) ZnO colloids and ZnO nanoparticles synthesized by pulsed laser ablation of zinc powders in water, Mater Sci Semicond Process. 109:104918.
- Bae SY, Seo HW, Park J (2020) Vertically Aligned Sulfur-Doped ZnO Nanowires Synthesized via Chemical Vapor Deposition, Chem in form, 35:30.
- Saravanakkumar D, Sivaranjani S, Kaviyarasu K, Ayeshamariam A, Ravikumar B, Pandiarajan S, Veeralakshmi C, Jayachandran M, Maaza M (2018) Synthesis and characterization of ZnO–CuO nanocomposites powder by modified perfume spray pyrolysis method and its antimicrobial investigation, J. Semicond. 39:033001.
- Bazazi S, Arsalani N, Khataee A, Tabrizi AG (2018) Comparison of ball milling-hydrothermal and hydrothermal methods for synthesis of ZnO nanostructures and evaluation of their photocatalytic performance, J. Ind. Eng. Chem. 62:265–272.
- Navas D, Ibañez A, González I, Palma JL, Dreyse P (2020) Controlled dispersion of ZnO nanoparticles produced by basic precipitation in solvothermal processes. Heliyon 6:e05821.
- Satheskumar M, Anand B, Muthuvel A, Rajarajan M, Mohana V, Sundaramanickam A (2020) Enhanced photocatalytic dye degradation and antibacterial activity of biosynthesized ZnO-NPs using curry leaves extract with coconut water, Nanotechnol Environ Eng 5(3).

17. Alavi M, Nokhodchi A (2021) Synthesis and modification of bio-derived antibacterial Ag and ZnO nanoparticles by plants, fungi, and bacteria, *Drug Discov Today* 26:1953–62.
18. Muthuvel A, Jothibas M, Manoharan C (2020) Synthesis of copper oxide nanoparticles by chemical and biogenic methods: photocatalytic degradation and in vitro antioxidant activity, *Nanotechnol. Environ. Eng* 5:(2).
19. Liu C, Leng W, Vikesland PJ (2018) Controlled Evaluation of the Impacts of Surface Coatings on Silver Nanoparticle Dissolution Rates, *Environ Sci Technol* 52:2726–34.
20. Ansari MA, Murali M, Prasad D, Alzohairy MA, Almatroudi A, Alomary MN, et al. (2020) Cinnamomum verum Bark Extract Mediated Green Synthesis of ZnO Nanoparticles and Their Antibacterial Potentiality, *Biomolecules* 10:336.
21. Elumalai K, Velmurugan S (2015) Green synthesis, characterization and antimicrobial activities of zinc oxide nanoparticles from the leaf extract of *Azadirachta indica* (L.), *Appl Surf Sci* 345:329–336.
22. Santhoshkumar J, Kumar SV, Rajeshkumar S (2017) Synthesis of zinc oxide nanoparticles using plant leaf extract against urinary tract infection pathogen, *Resource-Efficient Technologies*, 3:459–465.
23. Matinise M, Fuku XG, Kaviyarasu K, Mayedwa N, Maaza M, (2017) ZnO nanoparticles via *Moringa oleifera* green synthesis: Physical properties & mechanism of formation, *Appl Surf Sci* 406:339–347.
24. Chekuri S, Lingfa L, Panjala S, Bindu KCS, Anupalli RR (2020) *Acalypha indica* L. - an Important Medicinal Plant: A Brief Review of Its Pharmacological Properties and Restorative Potential, *European J Med Plants* ;1–10.
25. Sivaraj R, Rahman PKSM, Rajiv P, Narendhran S, Venckatesh R (2014) Biosynthesis and characterization of *Acalypha indica* mediated copper oxide nanoparticles and evaluation of its antimicrobial and anticancer activity, *Spectrochim Acta A Mol Biomol Spectrosc* 129:255–8.
26. Chinnathambi A, Vasantharaj S, Saravanan M, Sathiyavimal S, Duc PA, Nasif O, et al. (2021) Biosynthesis of TiO₂ nanoparticles by *Acalypha indica*; photocatalytic degradation of methylene blue, *Appl Nanosci*.
27. Krishnaraj C, Jagan EG, Rajasekar S, Selvakumar P, Kalaichelvan PT, Mohan N (2010) Synthesis of silver nanoparticles using *Acalypha indica* leaf extracts and its antibacterial activity against water borne pathogens, *Colloids Surf. B: Biointerfaces* 76:50–6.
28. Elayaraja M, Punithavathy IK, Jothibas M, Muthuvel A, Jeyakumar SJ (2020) Effect of rare-earth metal ion Ce³⁺ on the structural, optical and photocatalytic properties of CdO nanoparticles, *Nanotechnol. Environ. Eng* 5:3.
29. Ravichandran V, Sumitha S, Ning CY, Xian OY, Kiew Yu U, Paliwal N, et al. (2020) Durian waste mediated green synthesis of zinc oxide nanoparticles and evaluation of their antibacterial, antioxidant, cytotoxicity and photocatalytic activity, *Green Chem Lett Rev* 13:102–16.
30. Thiruselvi D, Yuvarani M, Amudha T, Sneha R, Mariselvam AK, Anil Kumar M, et al. (2018) Synthesis of iron nano-catalyst using *Acalypha indica* leaf extracts for biogas production from mixed liquor volatile suspended solids, *Energy Sources A: Recovery Util. Environ. Eff.* 40:772–9.
31. Wang N, Yang Y, Yang G (2011) Great blue-shift of luminescence of ZnO nanoparticle array constructed from ZnO quantum dots, *Nanoscale Res Lett* 6:1.
32. Jamdagni P, Khatri P, Rana JS (2018) Green synthesis of zinc oxide nanoparticles using flower extract of *Nyctanthes arbor-tristis* and their antifungal activity, *J King Saud Univ Sci* 30:168–75.
33. Ramasamy V, Mohana V, Suresh G (2018) Study of Ni-CeO₂ nanoparticles for efficient photodegradation of methylene blue by sun light irradiation, *Indian J Phys* 92:1601–12.
34. Vijayakumar S, Mahadevan S, Arulmozhi P, Sriram S, Praseetha PK (2018) Green synthesis of zinc oxide nanoparticles using *Atalantia monophylla* leaf extracts: Characterization and antimicrobial analysis, *Mater Sci Semicond Process* 82:39–45.
35. haudhuri SK, Malodia L (2017) Biosynthesis of zinc oxide nanoparticles using leaf extract of *Calotropis gigantea*: characterization and its evaluation on tree seedling growth in nursery stage, *Appl Nanosci* 7:501–12.
36. Sorbiun M, Shayegan Mehr E, Ramazani A, Taghavi Fardood S (2017) Biosynthesis of Ag, ZnO and bimetallic Ag/ZnO alloy nanoparticles by aqueous extract of oak fruit hull (Jaft) and investigation of photocatalytic activity of ZnO and bimetallic Ag/ZnO for degradation of basic violet 3 dye, *J Mater Sci Mater Electron* 29:2806–14.
37. Lalitha Phani AV, Srinivas B, Hameed A, Narasimha Chary M, Rao JL, Shareefuddin M (2019) Comparative studies on physical and spectroscopic properties of aluminobismuth borate glasses containing Pb, Zn & Cd ions, *Chin J Phys.* 58:303–19.
38. Mahendra C, Murali M, Manasa G, Ponnamma P, Abhilash MR, Lakshmeesha TR, Satish A, Amruthesh KN, Sudarshana MS (2017) Antibacterial and antimutagenic potential of bio-fabricated zinc oxide nanoparticles of *Cochlospermum religiosum* (L.), *Microb Pathog* 110:620–629.
39. Radzi AASM, Safaei J, Teridi MAM (2019) Photoelectrochemical enhancement from deposition of BiVO₄ photosensitizer on different thickness layer TiO₂ photoanode for water splitting application, *Nano-Struct. Nano-Objects* 18:100274.
40. Vadivel S, Rajarajan G (2015) Effect of Mg doping on structural, optical and photocatalytic activity of SnO₂ nanostructure thin films, *J Mater Sci Mater Electron* 26:3155–62.
41. Kumar M, Dubey S, Rajendar V, Park S-H (2017) Fabrication of ZnO Thin Films by Sol-Gel Spin Coating and Their UV and White-Light Emission Properties, *J Electron Mater* 46:6029–37.
42. Lallo da Silva B, Caetano BL, Chiari-Andréo BG, Pietro RCLR, Chiavacci LA (2019) Increased antibacterial activity of ZnO nanoparticles: Influence of size and surface modification, *Colloids Surf. B: Biointerfaces* 177:440–7.
43. Pai S, H S, Varadavenkatesan T, Vinayagam R, Selvaraj R (2019) Photocatalytic zinc oxide nanoparticles synthesis using *Peltophorum pterocarpum* leaf extract and their characterization, *Optik* 185:248–55.
44. Alamdari S, Sasani Ghamsari M, Lee C, Han W, Park H-H, Tafreshi MJ, et al. (2020) Preparation and Characterization of Zinc Oxide Nanoparticles Using Leaf Extract of

- Sambucus ebulus, Appl Sci 10:3620.
45. Shabaani M, Rahaiee S, Zare M, Jafari SM (2020) Green synthesis of ZnO nanoparticles using loquat seed extract; Biological functions and photocatalytic degradation properties, LWT 134:110133.
 46. Vinayagam R, Pai S, Varadavenkatesan T, Pugazhendhi A, Selvaraj R (2021) Characterization and photocatalytic activity of ZnO nanoflowers synthesized using Bridelia retusa leaf extract, Appl Nanosci
 47. Varadavenkatesan T, Lyubchik E, Pai S, Pugazhendhi A, Vinayagam R, Selvaraj R, (2019) Photocatalytic degradation of Rhodamine B by zinc oxide nanoparticles synthesized using the leaf extract of *Cyanometra ramiflora*, J Photochem Photobiol. B Biol 199:111621.
 48. A. B. Moghaddam, M. Moniri, S. Azizi, R. A. Rahim, A. B. Ariff, W. Z. Saad, F. Namvar, M. Navaderi, and R. Mohamad (2017) Biosynthesis of ZnO Nanoparticles by a New *Pichia kudriavzevii* Yeast Strain and Evaluation of Their Antimicrobial and Antioxidant Activities, Molecules 22: 872
 49. R. Dobrucka and J. Długaszewska (2016) Biosynthesis and antibacterial activity of ZnO nanoparticles using *Trifolium pratense* flower extract, Saudi Journal of Biological Sciences, 23: 517–523